Asian Journal of Chemistry; Vol. 34, No. 10 (2022), 2604-2610

ASIAN JOURNAL OF CHEMISTRY

https://doi.org/10.14233/ajchem.2022.23870

Characterization and Antibacterial Activity of Cu doped ZnO Thin Film Prepared by Sol-Gel Dip Coating Method and Phytosynthesized Zinc Oxide Nanoparticles from *Senna alata* and *Euphorbia hirta*

R. SUMALATHA[1,*], M. SIVAKUMAR[2] and G. PARTHASARATHY[3]

[1]Department of Physics, Jaya College of Arts and Science, Chennai-602024, India
[2]PG and Research Department of Physics, Presidency College, Chennai-600005, India
[3]Department of Electronics, Jaya College of Arts and Science, Chennai-602024, India

*Corresponding author: E-mail: sumalatha2688@gmail.com

Received: 17 April 2022; *Accepted*: 18 June 2022; *Published online*: 19 September 2022; AJC-20963

Zinc oxide nanoparticles exhibit significant antibacterial activity. The present study focused on determining the antibacterial activity of green synthetic zinc oxide nanoparticles (ZnO NPs) and Cu doped ZnO thin film. The prepared ZnO NPs and Cu doped ZnO films were characterized by XRD analysis, SEM, FTIR and UV-vis. Amorphous and nano cluster shapes were observed in SEM analysis. The presence of different chemical functional groups was confirmed by FTIR analysis. The optical properties Cu doped ZnO nanostructures were analyzed by UV-visible analysis. The results clearly confirmed the efficient synthesis of spherical ZnO nanoparticles with average size range from 40 to 50 nm. The Cu doped ZnO thin films and ZnO nanoparticles showed dose-dependent antibacterial activity against *Escherichia coli*, *Staphylococcus aureus*, *Bacillus subtilis*, *Salmonella typhi* and *Pseudomonas aeruginosa*. The IC_{50} value was calculated as approximately 60 µg/mL. Growth kinetics studies were performed in the presence of ZnO nanoparticles demonstrated the bacteriostatic effect of ZnO nanoparticles.

Keywords: *Senna alata*, *Euphorbia hirta*, Zinc oxide nanoparticles, Antibacterial activity.

INTRODUCTION

Zinc oxide is an immense metal oxide semiconductor. It has new scientific applications in different fields. ZnO has multifunctional features such as piezoelectric, electrophysics, catalysis and antibacterial activity [1]. ZnO is a semiconductor N-type extrinsic with wide narrow band and large exciton energy (3.3 eV and 60 meV) [2-4]. ZnO nanostructures are synthesized by different methods, such as solvent methods, sol-gel methods, hydrothermal methods, coprecipitating methods, heat evaporation techniques, chemical and physical vapour deposition and vapour transportation. ZnO is doped with different elements for the change of electrical and optical properties. The most common elements are doped with ZnO as Al, Ni, Fe, Mg, Co, Mn and Ce [5,6]. Among different factors, Cu has many physical, chemical and antibacterial properties with Zn.

Additional Cu in the ZnO network improves the microstructure and antibacterial attributes of ZnO [7,8]. ZnO is widely used in areas such as solar cells, biosensors and anticancer activities [8,9]. Different forms of ZnO nanostructures are nano, nanobelt and nanowire [10]. In which, ZnO thin films are fabricated by sol-gel dipping coating method. The prepared Cu-doped ZnO films were characterized by SEM, FTIR, UV-vis and XRD analysis. The morphological change of ZnO due to addition of Cu is reported. The antibacterial activity was determined by testing the growth inhibition of *S. typhi*, *S. aureus*, *B. subtilis*, *E. coli* and *P. aeruginosa*. The current study also explores the green route synthesis of zinc oxide nanoparticles from the green aqueous extracts of herbal plants *Senna alata* as well as *Euphorbia hirta*. The *in vitro* bioactivity studies of ZnO NPs synthesized from *Senna alata* were analyzed such that antibacterial activity was performed against Gram-positive and Gram-negative microorganism and compared with ZnO NPs synthesized from *E. hirta* for the similar activity. Inhibition zones of maximum 20 mm and 18 mm were obtained against *Escherichia coli* and *Pseudomonas aeruginosa* for *Senna alata* and *Euphorbia hirta*, respectively.

EXPERIMENTAL

Extraction: *Senna alata* and *Euphorbia hirta* were identified and authenticated by Botanical Survey of India (BSI), Southern circles, Government of India. The well-known fresh leaves of the plants were collected randomly from the region of Yercaud and Kolli hills, Eastern Ghats, India.

Methanol was used for extraction of plant sample. Air dried and powdered plant materials (30 g) were extracted with 300 mL of solvents by using Soxhlet apparatus for 10 h at a temperature not exceeding the boiling of the solvents. The obtained extracts were filtered using Whatman filter paper No. 1 and the filtrates were then evaporated in hot air oven at 100 ºC. The dried extracts were stored in air tight bottles for further use.

Green synthesis of ZnO nanoparticles: For the synthesis of ZnO powder, 50 mL of plant leaves extract was taken and boiled at 60-80 ºC by using a stirrer-heater. Then, 5 g of zinc nitrate was added to the solution as the temperature reaches 60 ºC. This mixture was then boiled until it is converted to a deep certain coloured suspension. This paste was then collected in a ceramic crucible and heated in an air heated furnace at 100 ºC for 1 h and then it was grained using a mortar and pestle. A light white coloured powder was obtained and this powder was carefully collected and sent for different characterizations.

Preparation of Cu doped ZnO thin films: In present work, Cu doped ZnO thin films have been prepared on to well cleaned glass substrates by simple sol gel dip coating method. Zinc acetate was used as zinc precursor and $Cu(NO_3)_2$ as a dopant for thin films. Zinc acetate was used as a starting material and deionized water was used as the solvent. Zinc acetate was first dissolved in deionized water and stirred for 30 min at room temperature. Doping solution was obtained in separate beaker by adding copper nitrate in deionized water. The mol percentage of dopant in the solution is 0.5 mol%. These two solutions were mixed and stirred for 2 h to yield a homogeneous solution and finally the solution was aged at room temperature for 24 h. The prepared Cu doped ZnO thin films were annealed at 450 ºC.

Qualitative phytochemical analysis: The qualitative phytochemical analysis of *Senna alata* and *Euphorbia hirta* was performed using methanol solvent. In *Senna alata* leaf methanol extract, the phytochemicals like alkaloids, flavonoids, steroids, anthroquinone, phenols, tannin and carbohydrates were present. Whereas saponins, oils and resins were absent in *Senna alata* extract.

The qualitative phytochemical analysis of *Euphorbia hirta* leaf methanol extract revealed the presence of alkaloids, flavonoids, terpenoids, phenols and carbohydrates. Steroids, anthroquinone, saponins, tannin are present whereas oils and resins were found to be absent.

Antibacterial activity: Stock cultures were maintained at 4 ºC on slopes of nutrient agar. Active cultures of experiment were prepared by transferring a loop full of cells from the stock cultures to test tube of Muller-Hinton broth (MHB) for *S. typhi*, *S. aureus*, *B. subtilis*, *E. coli* and *P. aeruginosa*, which were incubated without agitation for 24 h at 37 ºC and 25 ºC, respectively. The cultures were diluted with fresh Muller-Hinton broth to achieve optical densities corresponding to 2.0×10^6 colony forming units (CFU/mL) for bacteria.

XRD analysis: The structural properties of green synthesized ZnO nanoparticles and the sol gel Cu doped ZnO doped thin films have been studied, which was carried out using a XPERT-PRO with Cu$K\alpha$ radiation at the Bragg angle ranging from 20º to 80º. From this analysis, the lattice parameter, grain size, strain and dislocation density have been calculated. The elemental compositions and surface morphological analysis of the prepared samples have been studied using scanning electron microscope (Hitachi VP-SEM S-3400N).

FESEM analysis: Surface morphological and elemental compositions analysis of the prepared samples has been studied using field emission scanning electron microscope (EIGMA-VP).

UV-visible analysis: The absorbance and transmittance patterns of green synthesized ZnO nanoparticles and Cu doped ZnO thin films are investigated. The band gap of the samples was calculated using the formula $E = hc/\lambda$. The UV-vis spectrophotometer has been used to record the absorbance spectra of ZnO nanoparticles and Cu doped ZnO thin in the wavelength range of 200 to 800 nm and the results were discussed.

Antibacterial susceptibility test: The disc diffusion method was used to screen the antimicrobial activity. *In vitro* antimicrobial activity was screened by using Muller Hinton Agar (MHA) obtained from Hi-media (Mumbai). The MHA plates were prepared by pouring 15 mL of molten media into sterile petriplates. The plates were allowed to solidify for 5 min and 0.1% inoculums suspension was swabbed uniformly and the inoculums were allowed to dry for 5 min. The sterile discs of 6 mm were loaded with 20, 30, 40 and 50 µL of test solution (ZnO NPs). The loaded disc was placed on the surface of medium and the extract was allowed to diffuse for 5 min and the plates were kept for incubation at 37 ºC for 24 h. At the end of incubation, inhibition zones formed around the disc were measured in millimeter.

RESULTS AND DISCUSSION

XRD studies: Fig. 1a shows the XRD pattern of green synthesized ZnO nanoparticles prepared with *Senna alata* leaf extract at 70 ºC. The detected (*h k l*) peaks at 2θ values of 31.42º, 34.47º and 36.75º corresponding to the lattice planes (100), (002) and (101), respectively. They are in agreement with the standard JCPDS card no. 036-1451 for hexagonal Wurtzite ZnO. XRD pattern of the sample ZnO A exhibits all three diffraction peaks (100), (002) and (101) correspond to Wurzite ZnO with strong (002) diffraction peak compared with (100) and (101) peaks.

Similarly, Fig. 1b shows the XRD pattern of ZnO nanoparticles prepared with *Euphorbia hirta* leaf extract at 70 ºC. The detected (*h k l*) peaks at 2θ values of 31.43º, 34.46º and 36.62º correspond to the lattice planes (100), (002) and (101), respectively. They are in agreement with the standard JCPDS card no. 036-1451 card for hexagonal Wurtzite ZnO. The XRD pattern of sample ZnO A exhibits all three diffraction peaks (100), (002) and (101) correspond to the Wurzite ZnO with strong (002) diffraction peak compared with (100) and (101) peaks.

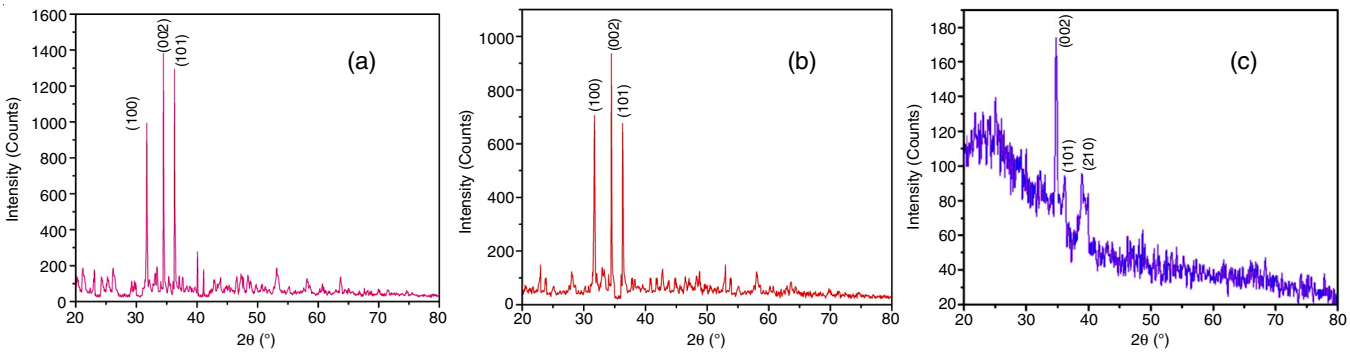

Fig. 1. X-ray diffraction patterns of ZnO NPs synthesized from (a) *Senna alata*, (b) *Euphorbia hirta* and (c) Cu doped ZnO thin film annealed at 450 °C

Fig. 1c shows the XRD pattern of Cu doped ZnO thin film annealed at 450 ºC. The diffraction peaks are indexed to primitive hexagonal Wurtzite structure and is in accordance with the JCPDS card no. 36-1451 with unit cell parameter a = 3.249 Å and c = 5.206 Å. The Cu doped ZnO thin film exhibits a very strong diffraction peak, indicating that the sample had a preferential orientation along the (002) plane. The structural parameters of green synthesized ZnO nanoparticles and Cu doped ZnO thin films are shown in Table-1. The grain size of the green synthesized ZnO nanoparticles was found to be 44.4, 44.6 nm and for Cu doped ZnO thin film the grain size was found to be 42.25 nm.

TABLE-1
GRAIN SIZES OF ZnO NPs WITH DIFFERENT PLANT EXTRACTS AND Cu DOPED ZnO THIN FILMS

Samples	2θ (°)	FWHM (°)	Grain size (nm)
ZnO NPs *Senna alata*	34.47	0.1968	44.4
ZnO NPs *Euphorbia hirta*	34.46	0.1968	44.6
Cu doped ZnO thin film	34.55	0.1968	42.25

Compared to greenly synthesized ZnO nanoparticles, Cu doped ZnO thin film has low peak intensity. It can be inferred that copper ions might inserted into the structure of ZnO and located at interstices or occupied some of the lattice sites of ZnO. The XRD studies indicated that hexagonal phase was probably the dominant one because typical reflections for the hexagonal phase appeared in the diffraction patterns and typical reflections for the cubic phase were not identified. It is found that undoped and Cu doped ZnO thin film had a high degree of c-axis orientation.

FESEM images: Fig. 2a-b shows the FESEM images of green synthesized ZnO nanoparticles. The FESEM images depict the surface texture and porosity of both synthesized ZnO nanoparticles from two different plants. The entire samples exhibit nanoclusters in the form of spheres. It is clear that ZnO nanoparticles has rough surface with heterogeneous porous nature. It indicates that there is good possibility for adsorption.

Fig. 2c shows the FESEM image of Cu doped ZnO thin film annealed at 450 ºC. By increasing the annealing temperature, the grains become denser and larger which can be considered as a coalescence process induced by the thermal treatment. The grain size increases with increasing annealing temperature from 350 to 450 ºC. Film annealed at 450 ºC shows the structure consisting of nanospheres of different sizes, uniformly dispersed throughout the film. As the annealing temperature increases the porosity of the film gets increased and the thin film prepared at 450 ºC shows a higher porosity.

EDAX studies: The EDAX spectra of the respective green route synthesized ZnO NPs are displayed in Fig. 3a-b. The EDAX spectra of Cu doped ZnO thin film annealed at 450 ºC are shown in Fig. 3c. From the EDAX results, it is confirmed that used chemicals were in the perfect combination of zinc oxide with atomic weightage of zinc and oxide. The amount of Zn and O obtained by EDAX analysis for *Senna alata* is 42.15% and 14.2%, respectively. For *Euphorbia hirta*, the amounts of Zn and O were 49.51% and 8.16%, respectively.

The amount of Zn, O and Cu obtained by EDAX analysis in Cu doped ZnO thin film was 45.94%, 48.20% and 1.36% respectively. The percentage of Zn, O and Cu elements available in the respective samples are shown in Table-2a and 2b.

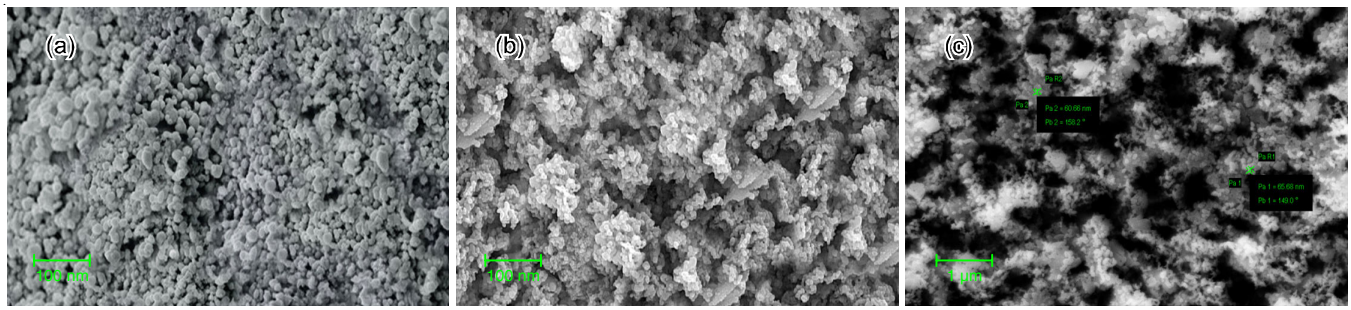

Fig. 2. FESEM images of green synthesized ZnO nanoparticles from (a) *Senna alata*, (b) *Euphorbia hirta* and (c) Cu doped ZnO thin film annealed at 450 °C

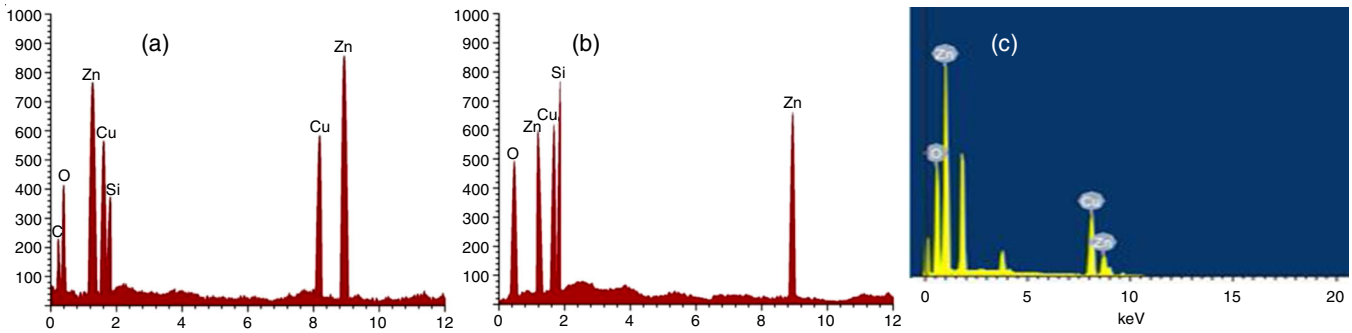

Fig. 3. EDAX Analysis of ZnO NPs synthesized from (a) *Senna alata*, (b) *Euphorbia hirta* and (c) Cu doped ZnO thin film annealed at 450 °C

TABLE-2
EDAX ANALYSIS OF GREEN SYNTHESIZED ZnO NPs USING FROM (a) *Senna alata* and (b) *Euphorbia hirta*

(a) *Senna alata*			(b) *Euphorbia hirta*		
Elements	Intensity	Weight (%)	Elements	Intensity	Weight (%)
C	0.16	4.34	O	0.25	14.27
O	0.25	8.16	Zn	1.23	20.69
Zn	1.23	23.72	Cu	1.56	19.98
Cu	1.56	15.21	Si	1.65	23.60
Si	1.65	7.01	Zn	8.97	21.46
Cu	8.13	15.77			
Zn	8.97	25.79			

The percentage of Zn (55.4%), O (43.20%) and Cu (1.36%) elements present in the Cu doped ZnO thin film.

FTIR studies: Fig. 4a shows the FTIR spectrum of green synthesized ZnO nanoparticles synthesized from *Senna alata* leaf extract. The characteristic peaks obtained at 3823 and 3527 cm^{-1} are assigned to O-H stretching while the peaks at 1994 and 17581 cm^{-1} are ascribed to O-H bending vibration. The characteristic peaks at 641 and 1064 cm^{-1} indicate the formation stretching mode of Zn-O bond. The occurrence of the above-mentioned functional groups proves the formation of ZnO.

Simiarly, Fig. 4b shows the FTIR spectrum of green synthesized ZnO nanoparticles from *E. hirta* leaf extract. The characteristic peaks were observed at 3241, 2927, 2841, 1709, 1513 and 738 cm^{-1}. The peaks at 3241 and 1709 cm^{-1} are assigned to O-H stretching and O-H bending vibrations, respectively. The characteristic peaks at 738 and 1086 cm^{-1} indicate the formation stretching mode of Zn-O bond. The formation of ZnO was authenticated by the availability of various chemical functional groups.

Fig. 4c shows the FTIR spectrum of Cu doped ZnO thin film annealed at 450 ºC. The peaks at 3440 and 1134 cm^{-1} are assigned to O-H stretching and O-H bending vibration. The characteristic peaks at 834 and 527 cm^{-1} indicated the formation of Cu-O bond and stretching mode of Zn-O bond. The presence of various chemical functional groups proves the formation of Cu doped ZnO.

UV-visible studies: Fig. 5a shows the UV-visible spectra of green synthesized ZnO nanoparticles wherein an absorption peak appears at 321 nm for *S. alata* plant extract and at 231 nm for *E. hirta* plant extract. The absorption region of green synthesized ZnO nanoparticles covers entirely the UV-visible and near IR region. Photo-ionization occurring in the semi-

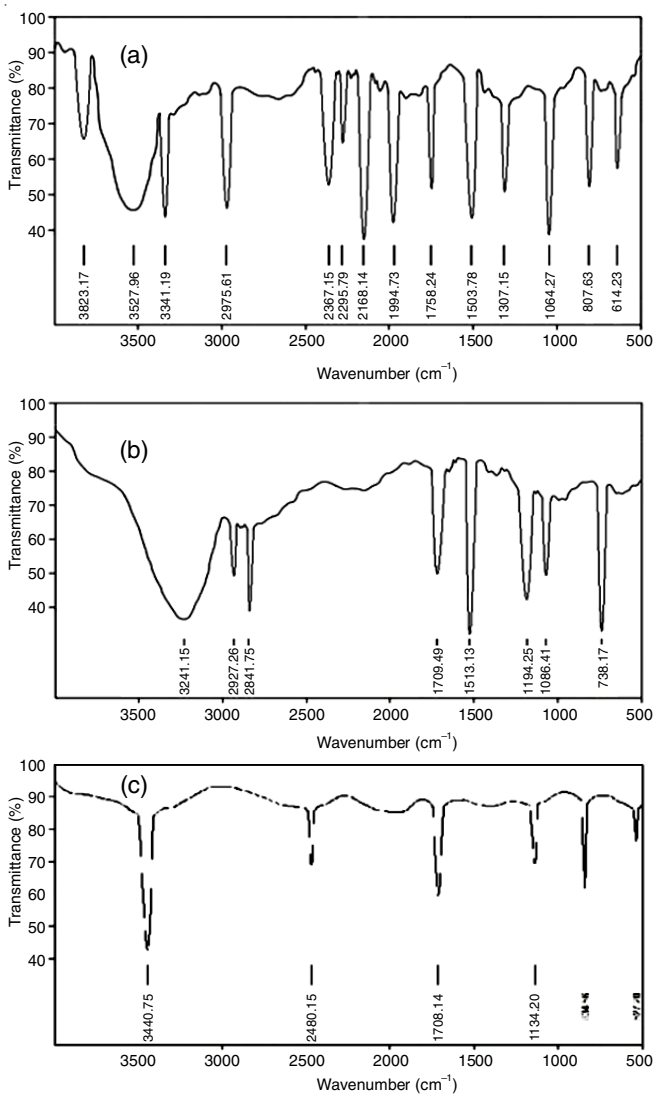

Fig. 4. FTIR spectrum of ZnO NPs synthesized from (a) *Senna alata*, (b) *Euphorbia hirta* and (c) Cu doped ZnO thin film annealed at 450 °C

conductor atoms lead to the occurrence of excitation for the valence electrons moving to the conduction band such that the required energy has to be either greater or equal to the bandgap value. Photo-ionization occurring in impurity atoms lead to the transition of electrons, which move either from the donor energy level to the conduction band or from the valence band to the acceptor level. Therefore, it is possible to use the UV

region for better analysis of antimicrobial activity. The values of optical band gap values have been measured by Tauc plot method (direct method). The obtained optical band gap value for *Senna alata* is 2.90 eV and for *Euphorbia hirta* is 3.00 eV. Fig. 5b shows the UV-vis absorption spectrum of Cu doped ZnO thin film annealed at 450 ºC. It can be seen that the absorption peak appears at 306 nm. The absorption region of prepared sample covers the UV and visible region. The obtained band gap value of Cu doped ZnO thin film was 2.9 eV.

UV-Vis transmittance spectra

Green synthesized ZnO nanoparticles: Fig. 6a shows UV-visible transmittance spectra of green synthesized ZnO nanoparticles of *Senna alata* and *Euphorbia hirta.* The optical transmittance of the ZnO nanoparticles is observed to be 21% for *Senna alata* and 41% for *Euphorbia hirta.*

Cu doped ZnO thin films: Fig. 6b shows the UV-vis transmittance spectrum of Cu doped ZnO thin film annealed at 450 ºC. It can be seen that the optical transmittance of Cu doped ZnO thin film is observed to be 19%. The bandgap values of green synthesized ZnO nanoparticles using *Senna alata* and *Euphorbia hirta* leaf extracts and Cu doped ZnO thin films are given in Table-3. It is obvious that the green synthesized ZnO samples and Cu doped ZnO exhibit smaller band gap and larger grain size and hence result in enhanced antibacterial activity. The Cu doped ZnO thin film exhibits more UV absorption due to their flower like structure depicted as depicted in FESEM (Fig. 2c). The illumination of ZnO thin films by UV light can also generate reactive species as superoxide radicals or hydroxyl radicals in an aqueous environment and it is used to degrade bacterial cell walls. The UV results suggest that green synthesized ZnO nanoparticles and Cu doped ZnO thin

TABLE-3
GRAIN SIZE AND BANDGAP VALUES
OF PREPARED ZnO SAMPLES

Samples	Grain size (nm)	Bandgap (eV)
ZnO (*Senna alata*)	44.4	2.90
ZnO (*Euphorbia hirta*)	44.6	3.00
Cu doped ZnO	42.25	2.90

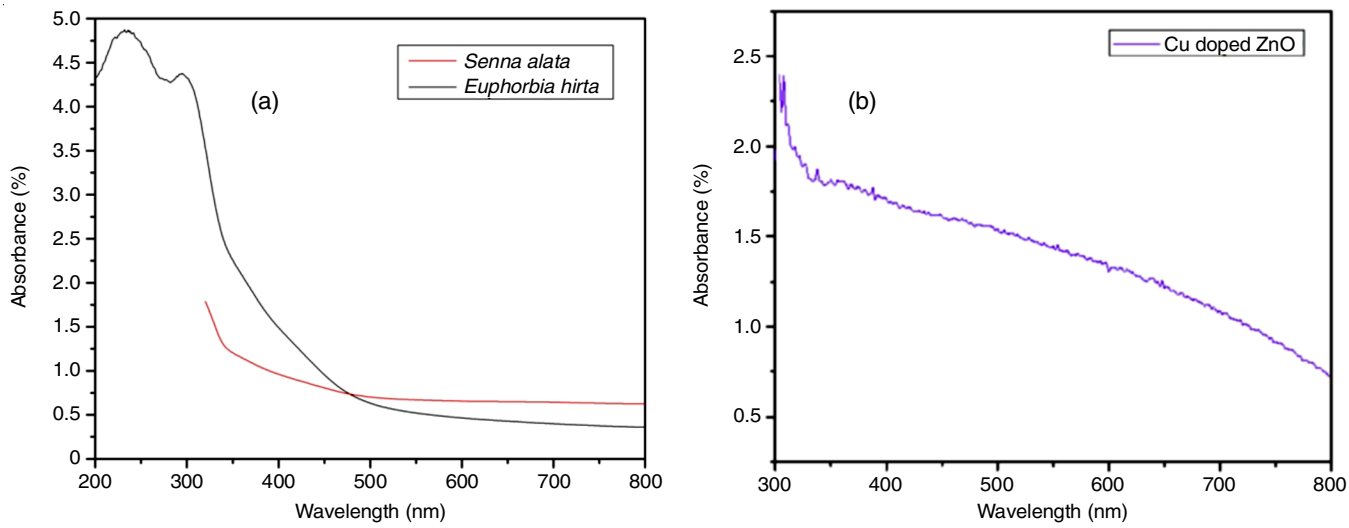

Fig. 5. UV-vis absorbance spectra of (a) green synthesized ZnO nanoparticles and (b) Cu doped ZnO thin film annealed at 450 °C

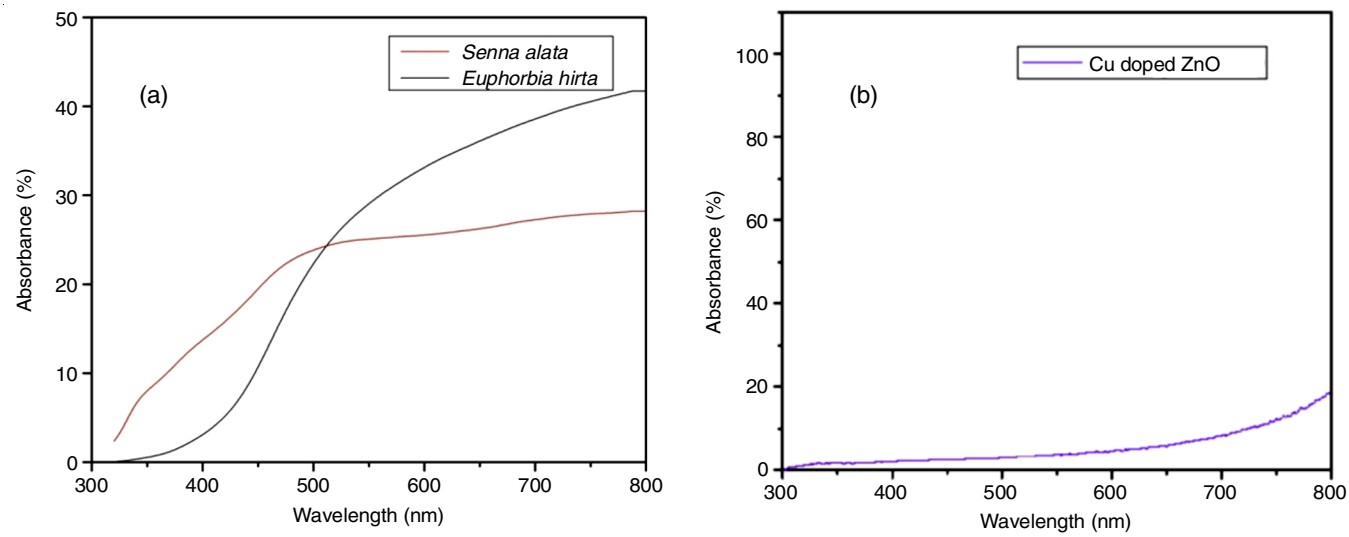

Fig. 6. UV-vis transmittance spectra of (a) green synthesized ZnO nanoparticles and (b) Cu doped ZnO thin film annealed at 450 °C

films could be promising potential candidates for antibacterial activity.

Natural substances extracted from plants have recently been considered as potential sunscreen resources because of their ultraviolet ray absorption in the UVA and B region and their antioxidant activity. There is strong evidence that DNA-damaging ultraviolet (UV) light induces the accumulation of UV light-absorbing flavonoids and other phenolics in dermal tissue of the plant body which are having excellent antioxidant and photo protective properties, hence can be exploited as a safe and effective ingredient in sunscreen lotions.

Antibacterial activity: The antibacterial activity of the synthesized ZnO nanoparticles from *Senna alata* towards Gram-positive and Gram-negative bacteria were screened by disc diffusion method. The synthesized ZnO nanoparticles obtained from the methanol extract of *Senna alata* show comparatively better effect as it comes against *P. aeruginosa*, *E. coli*, *S. aureus* and *B. subtilis*. The maximum zone of inhibition was observed for *P. aeruginosa* (20 mm), *E. coli* (20 mm), while the other zones of inhibition were *S. aureus* (19 mm), *B. subtilis* (18 mm) and *S. typhi* (17 mm) in 60 µL concentration. The antibacterial activity obtained *in vitro* reveals that the green synthesized extract has considerable activity against all the studied micro-organisms.

Similarly, the antibacterial activity obtained for the synthesized ZnO nanoparticles from methanol extract of *Euphorbia hirta* show fairly good impact against *P. aeruginosa*, *E. coli*, *S. aureus* and *S. typhi*. The observed maximum for the zone of inhibition appears to be for *P. aeruginosa* (18 mm) while the other zones of inhibition are observed for *E. coli* (17 mm), *S. aureus* (17 mm), *S. typhi* (15 mm) and *B. subtilis* (14 mm) in 60 µL.

The Cu doped ZnO thin film showed significant results when compared to ZnO thin films. As seen in Table-4, Cu doped ZnO thin film annealed exhibit lower inhibition in 20, 30 and 40 µL of concentration. The maximum zone of about 22 mm against *E. coli*, 21 mm against *B. subtilis*, 19 mm against *P. aeruginosa*, 18 mm against *S. aureus* and 17 mm against *S. typhi* was observed in 50 µL of concentration. This is because of the firm attachment of ZnO nanoparticles to the outer cell wall membrane of the bacteria. After that, ZnO nanoparticles begin to release oxygen species into the medium (bacteria), which inhibit the growth of cell leading to the distortion and leakage of the cell and finally the death of the cell [11]. The zone of inhibition which clearly indicates the mechanism of the biocidal action of the copper doped ZnO destroys the outer of the bacteria and leads to the death [12]. When compared to standard control, lower antibacterial activity of Cu doped ZnO thin film was observed in all the bacterial pathogens (Table-4). The observed difference in the diameter of the inhibition zone may be due to the difference in the susceptibility of different bacteria to the prepared ZnO nanoparticles [13].

Comparison of inhibition zone on 60 µL of concentration prepared ZnO samples shown in Fig. 7. The antibacterial activity of both green synthesized ZnO nanoparticles and Cu doped ZnO thin films were studied against the Gram-negative and the Gram-positive bacteria. The maximum inhibition zones of 22 mm, 21 mm, 19 mm, 17 mm and 20 mm were obtained for ZnO nanoparticles synthesized using *Senna alata* and Cu doped ZnO against all the five organisms *i.e. E. coli*, *B. subtilis*, *S. aureus*, *S. typhi* and *P. aeruginosa*, respectively.

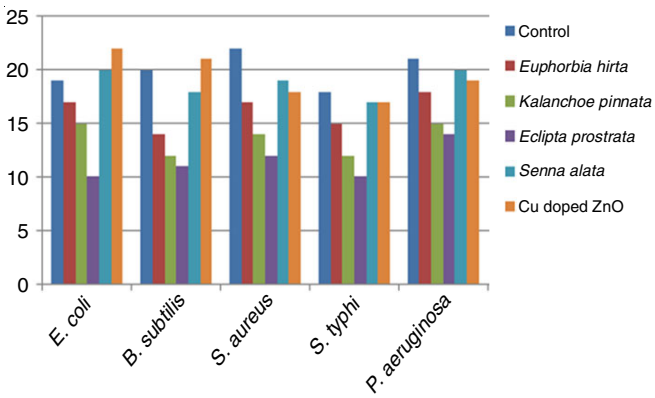

Fig. 7. Comparison of inhibition zone on 60 µL concentration of prepared ZnO samples

Hence, it is shown that the green synthesized ZnO nanoparticles and Cu doped ZnO thin films constitute an effective antimicrobial agent against pathogenic microorganisms. They act as potential candidates in the field of energy and medicine. In case of Cu doped ZnO thin films, the effect of both copper and zinc oxide has been established which in turn increases the antimicrobial effect of doped thin films. The antimicrobial effect of Cu doped ZnO thin films are because of the fact that metal complexes increase the intracellular reactive oxygen species (ROS). The produced ROS inhibit the intracellular enzymes of the microorganisms, thereby inhibiting microbial growth.

A comparative analysis of antibacterial activity of ZnO nanoparticles against *E. coli* reported by various researchers is shown in Table-5. These results indicate that the Green synthesized ZnO nanoparticles and Cu doped ZnO thin films exibit the better antibacterial activity. Thus, the results of the

TABLE-4
ANTIBACTERIAL ACTIVITY OF ZNO NANOPARTICLES SYNTHESIZED FROM *Senna alata* AND *Euphorbia hirta* AND Cu DOPED ZnO THIN FILM

Organisms	Control (mm)	Zone of inhibition (mm)				
		Euphorbia hirta	*Kalanchoe pinnata*	*Eclipta prostrata*	*Senna alata*	Cu doped ZnO
Escherichia coli	19	17	15	10	20	22
Bacillus subtilis	20	14	12	11	18	21
Staphylococcus aureus	22	17	14	12	19	18
Salmonella typhi	18	15	12	10	17	17
Pseudomonas aeruginosa	21	18	15	14	20	19

TABLE-5
INHIBITORY ZONE ON MINIMUM CONCENTRATION OF ZnO NANOPARTICLES AGAINST *E. coli* BACTERIA REPORTED BY VARIOUS RESEARCHERS

ZnO nanoparticles Sample	Zone of inhibition (mm) against *E. coli* bacteria	Ref.
Senna alata	11	[14]
Senna alata	10	[15]
Senna alata	09	[16]
Euphorbia hirta	13	[17]
Euphorbia hirta	19	[18]
Euphorbia hirta	15	[19]
Cu doped ZnO thin film	21	[20]
Cu doped ZnO thin film	12	[21]
Cu doped ZnO thin film	11	[22]
Senna alata	20	Present work
Euphorbia hirta	17	Present work
Cu doped ZnO thin film	22	Present work

present work are encouraging with green synthesis and it can be taken for further research.

Conclusion

In present study, ZnO nanoparticles were synthesized from two different *Senna alata* and *Euphorbia hirta* plant extracts using green combustion method. The Cu doped ZnO thin films were prepared using sol-gel dip-coating method. The prepared ZnO samples were characterized using XRD, FESEM, EDAX, FTIR and UV-visible techniques. The antibacterial activity of both green synthesized ZnO nanoparticles and Cu doped ZnO thin films were studied against the Gram-negative and the Gram-positive bacteria. Based on the obtained results, it was demonstrated that the green synthesized ZnO nanoparticles and Cu-doped ZnO thin film is an effective antibacterial agent against pathogenic microorganisms.

ACKNOWLEDGEMENTS

A continuous help and cooperation from Alagappa University, Karaikudi, South Indian Textile Research Association (SITRA), Coimbatore and Alpha-Omega Hi-Tech Bioresearch Centre, Salem, India in characterizing the samples are gratefully acknowledged.

CONFLICT OF INTEREST

The authors declare that there is no conflict of interests regarding the publication of this article.

REFERENCES

1. A. Kolodziejczak-Radzimska and T. Jesionowski, *Materials*, **7**, 2833 (2014); https://doi.org/10.3390/ma7042833
2. D. Sharma, S. Sharma, B.S. Kaith, J. Rajput and M. Kaur, *Appl. Surf. Sci.*, **257**, 9661 (2011); https://doi.org/10.1016/j.apsusc.2011.06.094
3. W. Feng, P. Huang, B. Wang, C. Wang, W. Wang, T. Wang, S. Chen, R. Lv, Y. Qin and J. Ma, *Ceram. Int.*, **42**, 2250 (2016); https://doi.org/10.1016/j.ceramint.2015.10.018
4. R. Mohan, K. Krishnamoorthy and S.J. Kim, *Chem. Phys. Lett.*, **539–540**, 83 (2012); https://doi.org/10.1016/j.cplett.2012.04.054
5. S. Muthukumaran and R. Gopalakrishnan, *Opt. Mater.*, **34**, 1946 (2012); https://doi.org/10.1016/j.optmat.2012.06.004
6. S.A. Khayatian, A. Kompany, N. Shahtahmassebi and A.K. Zak, *Ceram. Int.*, **42**, 110 (2016); https://doi.org/10.1016/j.ceramint.2015.08.008
7. R. Kumar, A. Umar, G. Kumar, M.S. Akhtar, Y. Wang and S.H. Kim, *Ceram. Int.*, **41**, 7773 (2015); https://doi.org/10.1016/j.ceramint.2015.02.110
8. M.F. Al-Ajmi, A. Hussain and F. Ahmed, *Ceram. Int.*, **42**, 4462 (2016); https://doi.org/10.1016/j.ceramint.2015.11.133
9. L. Zhifeng, L. Chengcheng, Y. Jing and E. Lei, *Solid State Sci.*, **12**, 111 (2010); https://doi.org/10.1016/j.solidstatesciences.2009.10.014
10. C.Y. Jiang, X.W. Sun, G.Q. Lo, D.L. Kwong and J.X. Wang, *Appl. Phys. Lett.*, **90**, 263501 (2007); https://doi.org/10.1063/1.2751588
11. Y. Liu, L. He, A. Mustapha, H. Li, Z.Q. Hu and M. Lin, *J. Appl. Microbiol.*, **107**, 1193 (2009); https://doi.org/10.1111/j.1365-2672.2009.04303.x
12. K.S. Siddiqi, A. ur Rahman, Tajuddin and A. Husen, *Nanoscale Res. Lett.*, **13**, 141 (2018); https://doi.org/10.1186/s11671-018-2532-3
13. N. Babayevska, L. Przysiecka, I. Iatsunskyi, G. Nowaczyk, M. Jarek, E. Janiszewska and S. Jurga, *Sci. Rep.*, **12**, 8148 (2022); https://doi.org/10.1038/s41598-022-12134-3
14. H. Agarwal, Happy, S. Menon, S.V. Kumar, S.R. Kumar, R.D. Sheba, T. Lakshmi and V.D. Nallaswamy, *Biochem. Biophys. Rep.*, **17**, 208 (2019); https://doi.org/10.1016/j.bbrep.2019.01.002
15. M.N. Somchita, I. Reezal, I.E.Nura and A.R. Mutalib, *J. Ethnopharmacol.*, **84**, 1 (2003); https://doi.org/10.1016/S0378-8741(02)00146-0
16. O. Adedayo, W.A. Anderson, M. Moo-Young, V. Snieckus, P.A. Patil and D.O. Kolawole, *Pharm. Biol.*, **39**, 408 (2008); https://doi.org/10.1076/phbi.39.6.408.5880
17. A. Annamalai, V.L.P. Christina, D. Sudha, M. Kalpana and P.T.V. Lakshmi, *Colloids Surf. B*, **108**, 60 (2013); https://doi.org/10.1016/j.colsurfb.2013.02.012
18. E.-M.M. Abubakar, *J. Med. Plants Res.*, **3**, 498 (2009).
19. G. Singh and P. Kumar, *Int. J. Appl. Basic Med. Res.*, **3**, 111 (2013); https://doi.org/10.4103/2229-516X.117082
20. M.M. Khan, M.H. Harunsani, A.L. Tan, M. Hojamberdiev, Y.A. Poi and N. Ahmad, *BioNanoSci.*, **10**, 1037 (2020); https://doi.org/10.1007/s12668-020-00775-5
21. M.K. Debanath, R.K. Saha, S.M. Borah, E. Saikia and K.K. Saikia, *Adv. Mater. Proc.*, **3**, 36 (2018); https://doi.org/10.5185/amp.2018/721
22. D.T. Handago, E.A. Zereffa and B.A. Gonfa, *Open Chem.*, **17**, 246 (2019); https://doi.org/10.1515/chem-2019-0018